

# Polarization of $\Lambda$ -hyperons, vorticity and helicity structure in heavy-ion collisions

A. V. Zinchenko, O. V. Teryaev, M. I. Baznat

P. G. Demidov Yaroslavl State University, Yaroslavl, Russia;  
JINR, Dubna, Russia

The European Physical Society Conference on High Energy Physics  
(EPS-HEP 2021), DESY, Hamburg, Germany, 26–30 July 2021

# Outline

- 1 Introduction
- 2 PHSD model
- 3 Vorticity structure
- 4 Helicity separation
- 5 Polarization
- 6 Summary

## Introduction

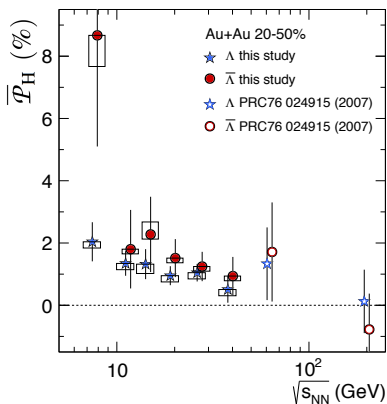


Fig: 1. The average polarization  $\bar{P}_H$ , where  $H = \Lambda$  or  $\bar{\Lambda}$ , from 20–50% central Au+Au collisions is plotted as a function of collision energy  $\sqrt{s_{NN}}$  (STAR Collab., Nature 548 (2017) 62–65)

# PHSD model

- The Parton-Hadron-String Dynamics (PHSD) (W. Cassing, E. L. Bratkovskaya, Phys. Rev. C78 (2008) 034919, arXiv:0808.0022 [hep-ph]) is the microscopic off-shell transport approach that consistently describes the full evolution of a relativistic heavy-ion collision from the initial hard scatterings and string formation through the dynamical deconfinement phase transition to the quark-gluon plasma as well as hadronization and to the subsequent interactions in the hadronic phase
- To calculate the vorticity field, the velocity field  $\vec{v}(x)$  needs to be known. In relativistic system, its definition is not unique. Several types of velocity field,  $\vec{v}_1$ ,  $\vec{v}_2$ , and  $\vec{v}_3$ , are introduced:

$$v_1^a(x) = \frac{\sum_i p_i^a F(x, x_i)}{\sum_i p_i^0 F(x, x_i)},$$

$$v_2^a(x) = \frac{1}{\sum_i F(x, x_i)} \sum_i \frac{p_i^a}{p_i^0} F(x, x_i),$$

$$v_3^a(x) = \frac{\sum_i p_i^a F(x, x_i)}{\sum_i [p_i^0 + (p_i^a)^2 / p_i^0] F(x, x_i)},$$

where  $a = 1, 2, 3$  are the spatial indices,  $p_i^a$  and  $p_i^0$  are the momentum and energy of the  $i$ -th particle, and the summation is over all the particles.

- The first definition,  $\vec{v}_1$ , is used in the following.

# Vorticity structure

- Similar to the velocity, several definitions of the vorticity exist
- Non-relativistic and relativistic kinetic vorticities:

$$\varpi_{\mu\nu} = \frac{1}{2}(\partial_\nu v_\mu - \partial_\mu v_\nu), \quad \omega_{\mu\nu} = \frac{1}{2}(\partial_\nu u_\mu - \partial_\mu u_\nu),$$

where  $u_\nu$  is a four-vector of the relativistic velocity field:

$$u^\nu(t, \vec{x}) = \gamma(t, \vec{x}) (1, \vec{v}(t, \vec{x})), \quad \gamma(t, \vec{x}) = \frac{1}{\sqrt{1 - \vec{v}^2(t, \vec{x})}}$$

- In the case of the relativistic vorticity,  $\gamma$ -factor has a significant influence on the fireball boundaries, strengthening vorticity value as shown in Fig. 2

# Vorticity structure

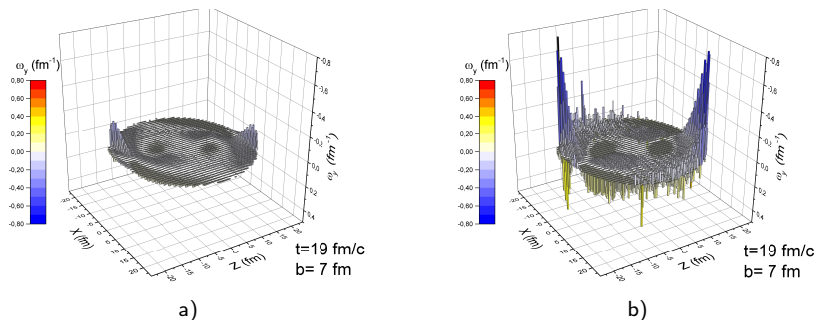
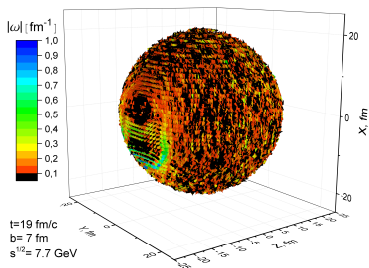


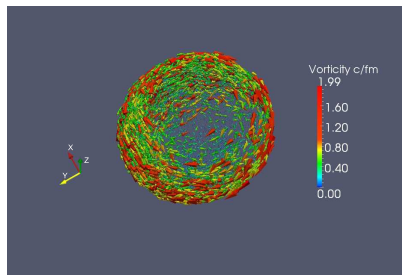
**Fig: 2.** Y-projection of the vorticity  $\vec{\omega}$  in the reaction plane  $xz$  ( $y = 0$ ) in the case of the non-relativistic (left plot a) and relativistic (right plot b) definitions at the energy  $\sqrt{s} = 7.7$  GeV

It takes the largest value on the boundaries of the fireball and spectators, and it has the same sign on both boundaries, which together gives a non-zero  $\omega_y$  vorticity

# Vorticity structure



a)



b)

Fig: 3. Vortex sheet in the PHSD (plot a) and QGSM (plot b) models

Since  $15 \text{ fm}/c$  the so-called vortex sheet begins to form on the boundary of the fireball at the energy  $\sqrt{s} = 7.7 \text{ GeV}$ . It is observed both in the Quark-Gluon String Model (QGSM) and PHSD model. In the PHSD model, the structure has a significant vorticity on the border of participants and spectators as shown in Figs. 2b and 3

# Vorticity structure

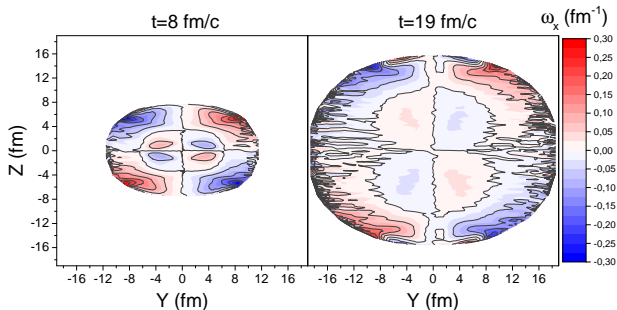


**Fig: 4.** Quadrupole structure of relativistic vorticity  $\omega_x$  in Au+Au at  $\sqrt{s} = 7.7$  GeV,  $x = 0$ , impact parameter  $b = 7$  fm

The presence of a vortex sheet in the perpendicular plane  $zy$  is seen. An increase in the  $x$ -projection of vorticity is observed around the boundary of the fireball and there are maximums at the boundary with spectators, as in plane  $xz$ . In addition, a mirror quadrupole structure with an internal part having an opposite sign with respect to the corresponding external region is also seen



# Vorticity structure

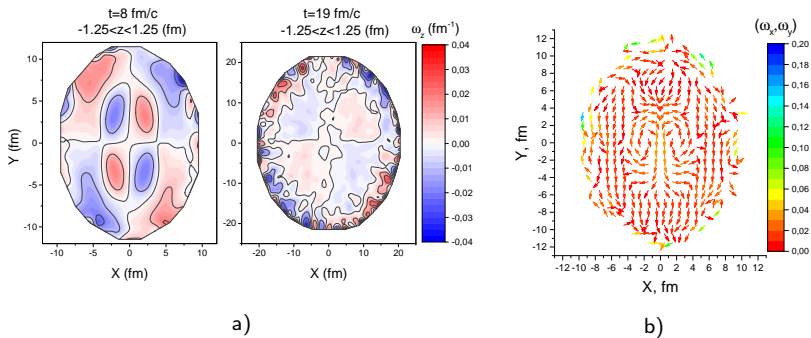


**Fig: 5.** a) Quadrupole structure of relativistic vorticity  $\omega_z$  in Au+Au at  $\sqrt{s} = 7.7 \text{ GeV}$  at the times  $t = 8 \text{ fm}/c$  and  $t = 19 \text{ fm}/c$ . Averaging is performed in the 2.5 fm range in the layer  $z = 0$ . b) Structure of the transverse vorticity  $\vec{\omega}_\perp = (\omega_x, \omega_y)$  in Au+Au at  $\sqrt{s} = 7.7 \text{ GeV}$ ,  $t = 8 \text{ fm}/c$ , and  $b = 7 \text{ fm}$  in the center of the fireball  $z = 0$ .

# Vorticity structure

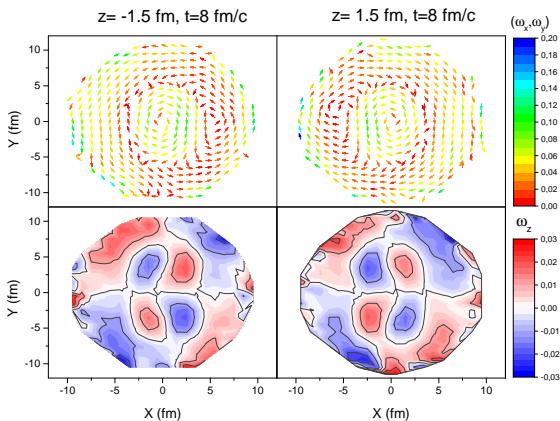


**Fig: 6.** Quadrupole structure of relativistic vorticity  $\omega_z$  in Au+Au at  $\sqrt{s} = 7.7$  GeV in the bottom line and corresponding structure of the transverse vorticity  $\vec{\omega}_{\perp} = (\omega_x, \omega_y)$  in the same time and layer of  $z$

# Vorticity structure

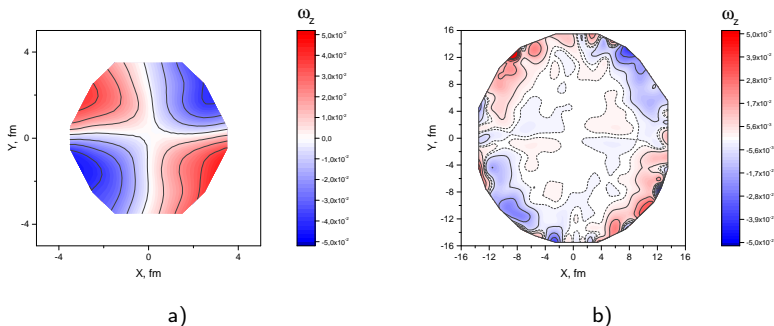


**Fig: 7.** Quadrupole structure of relativistic vorticity  $\omega_z$  in Au+Au at  $\sqrt{s} = 7.7$  GeV, impact parameter  $b = 8$  fm, and times  $t = 9.5$  fm/c (left plot) and  $t = 13$  fm/c (right plot) without  $p - p$  potential. Averaging is performed in the 5 fm range in the layer  $z = 0$

# Vorticity structure

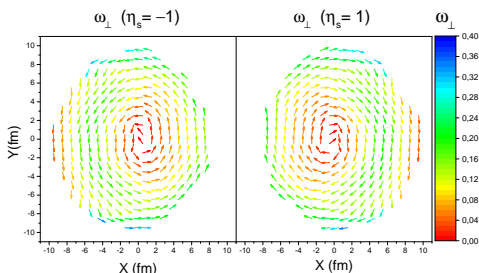


**Fig. 8.** The distribution of the transverse vorticity  $\vec{\omega}_\perp = (\omega_x, \omega_y)$  in the transverse plane at longitudinal position  $\eta_s = -1$  (left panel) and  $\eta_s = 1$  (right panel), where  $\eta_s = (1/2) \ln [(t+z)/(t-z)]$  is the space-time rapidity, at the time  $t = 9.5 \text{ fm}/c$ , impact parameter  $b = 5 \text{ fm}$  and energy  $\sqrt{s} = 7.7 \text{ GeV}$

It is consistent with the work (De-Xian We et al., Phys. Rev. C99 (2019) 014905, arXiv:1810.00151 [nucl-th]), where similar structures for the thermal vorticity at the same  $\eta_s$  are obtained.

# Vorticity structure

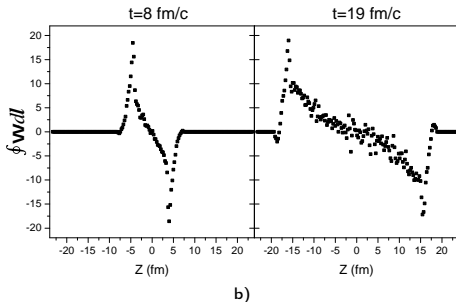
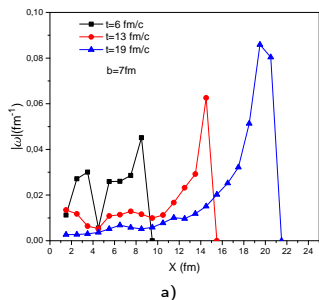


**Fig. 9.** a) Dependence of the vorticity modulus on the fireball radius at different times ( $b = 7$  fm,  $z = 0$ ,  $\sqrt{s} = 7.7$  GeV). b) Vorticity field circulation in the XY plane as a function of  $z$  in different time.

# Helicity separation

Helicity contributes directly to the polarization of hyperons

$$\langle \Pi_0^\Lambda \rangle = \langle \frac{m_\Lambda}{N_\Lambda p_y} \rangle \frac{N_c}{2\pi^2} \int d^3x \mu_s^2(x) \gamma^2 \epsilon^{ijk} v_i \partial_j v_k,$$

in the so-called axial vortical effect approach. The effect is proportional to vorticity and helicity of the strong interacting medium, and, in particular, to helicity separation effect discovered in the kinetic QGSM by M. Baznat et al. (Phys. Rev. C88 (2013) 061901; arXiv:1301.7003 [nucl-th]). The hydrodynamic helicity is contained within the integral  $H \equiv \int d^3x (\vec{v} \cdot \vec{\omega})$ . Helicity separation effect receives the significant contribution  $\sim v_y \omega_y$  from the transverse components of velocity and vorticity. It is easily explained by the same signs of transverse vorticities in the “upper” and “lower” (w.r.t. reaction plane) half-spaces, combined with the opposite signs of velocities. Even larger contribution of longitudinal components of velocity and vorticity,  $\sim v_z \omega_z$ , implies the appearance of the “quadrupole” structure of longitudinal vorticity.

# Helicity separation in the PHSD model

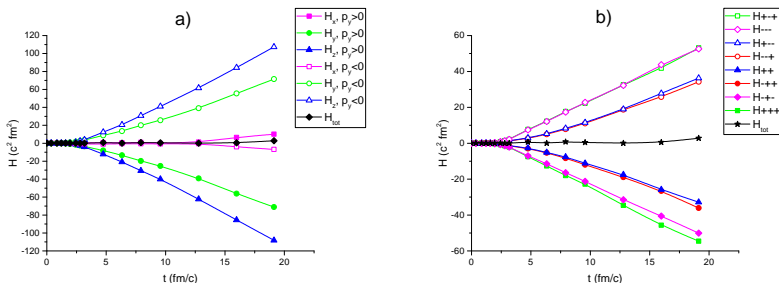


**Fig:** 10. a) Helicity  $H$  ( $\text{fm}^2 c^2$ ) separation relative to  $y$ -component of momentum (impact parameter  $b = 7$  fm and energy  $\sqrt{s} = 7.7$  GeV). b) Helicity  $H$  ( $\text{fm}^2 c^2$ ) separation relative to spatial octants ( $b = 7$  fm and  $\sqrt{s} = 7.7$  GeV), “+++” means that integration is performed in the octant  $x > 0, y > 0, z > 0$ , “---” is in the opposite octant  $x < 0, y < 0, z < 0$  and etc.

# Polarization of $\Lambda$ -Hyperons

The polarization of  $\Lambda$ -hyperons is calculated within the approach exploring local equilibrium thermodynamics (F. Becattini et al., Eur. Phys. J. C75 (2015) 191; arXiv:1403.6265 [hep-th]) and in the axial vortical effect approach with  $b = 7$  fm, energy  $\sqrt{s} = 7.7$  GeV and rapidity  $|y| < 1$ , where  $y = (1/2) \ln((E + p_z)/(E - p_z))$ . In thermodynamic approach, the spin vector  $\vec{S}^*$  averaged over the  $\vec{p}_\Lambda$  direction is determined by

$$\langle \vec{S}_\Lambda^* \rangle_{\vec{n}_p} = \frac{(1 - n_\Lambda)}{4M_\Lambda} \left( E_\Lambda + \frac{1}{3} \frac{\vec{p}_\Lambda^2}{E_\Lambda + m_\Lambda} \right) \text{rot} \vec{\beta}.$$

where  $\vec{\beta} = \vec{v}/T$  is thermodynamical velocity. The results for  $\Pi_0^\Lambda = 2 \langle S_{\Lambda y}^* \rangle_{\vec{n}_p}$  are  $\Pi_0^\Lambda = 0.7\%$  for thermodynamic approach and  $\Pi_0^\Lambda = 8\%$  for anomaly one, of which the last is very sensitive to chemical potential. The order of magnitude difference can be related firstly in the choice of velocity definition and secondly in the sensitivity to thermodynamic quantities.



# Summary

- 1 Simulations of Au-Au collisions in the PHSD model are performed. The structure of vorticity field of a collisional medium is studied.
- 2 Helicity separation effect is discovered in the PHSD model.
- 3 The values of  $\Lambda$ -hyperons polarization in the thermodynamic and axial vortical effect approaches are calculated.

# Backup

## Polarization

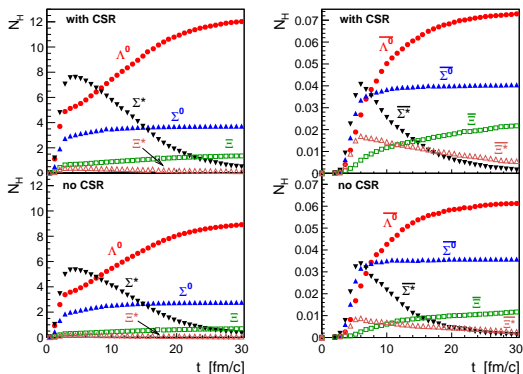


**Fig: 11.** Average numbers of strange particles (left panel) and anti-particles (right panel) as functions of collision time for Au+Au ( $\sqrt{s} = 7.7$  GeV) with the impact parameter  $b = 7.5$  fm. The upper panels correspond to the results calculated with and the bottom ones without the chiral symmetry restoration effect. (arXiv:1801.07610v1)